Electron Plasma Confinement in a Partially Toroidal Trap

M.R. Stoneking, P.W. Fontana, R.L. Sampson, and D.J. Thuecks

Department of Physics, Lawrence University, Appleton, WI 54911

Abstract. A new experiment seeks to examine equilibrium, stability, and confinement properties of toroidal electron plasmas. Electron plasmas with density about 3×10^6 cm^{-3} are trapped for ~ 100 μs in a "partially" toroidal (or 'C'-shaped) trap ($B \approx 200$ G). Large amplitude oscillations are observed in the 100 kHz frequency range. The oscillation frequency is proportional to $1/B$ and depends on the applied horizontal electric field, but not on the amount of charge in the trap. Some evidence points toward the ion resonance instability as the cause of these oscillations.

INTRODUCTION

Theory supports the expectation that equilibria exist for nonneutral plasmas in a toroidal magnetic field [1, 2, 3, 4]. Under certain restrictions, the equilibria are also expected to be stable [5, 6, 7]. Experiments confirm the existence of equilibria [8, 9, 10, 11], but to date, no experiment has tested the theory closely.

In this paper we report first measurements from a new experiment that seeks to explore toroidal equilibrium, stability and confinement of pure electron plasmas. Controlled injection of charge into the toroidal field is a significant initial hurdle to successful trapping of a nonneutral plasma. Past experimenters focused significant effort toward solving this problem [8, 9, 10, 11], but none of them achieved the kind of reproducible initial charge distributions routinely obtained in cylindrical traps. The present experiment provides controlled charge injection by limiting the confinement region to a 'C'-shaped segment of the torus. Charge is loaded directly onto field lines tied to the *partially* toroidal trapping region.

TOROIDAL EQUILIBRIUM

A toroidal magnetic field is nonuniform in magnitude and possesses curvature. The field can be written as

$$\mathbf{B} = \frac{B_o R_o}{R}\hat{\phi}, \tag{1}$$

where R is the distance from the major axis (major radial coordinate), R_o is the major radius of the plasma, B_o is the magnetic field at the center of the plasma, and $\hat{\phi}$ is the unit vector in the toroidal (azimuthal) direction. In the absence of other fields, charged particle guiding centers drift in the z-direction (vertically in most experimental configurations) due to the ∇B-drift and the curvature-drift. Circulation in the poloidal

CP606, *Non-Neutral Plasma Physics IV*, edited by F. Anderegg et al.

plane superimposed on the cross-field drifts can close the drift orbits. In the tokamak (and other toroidal quasineutral plasma devices), poloidal circulation of particles is ensured by giving the field a rotational transform, a poloidal field component generated by a toroidal plasma current. Field lines are then toroidal helices and particles circulate in the poloidal plane as a result of flow parallel to **B**.

By contrast, the hope for establishing closed drift orbits in a toroidal *nonneutral* plasma rests on the presence of the space charge electric field. A toroidal nonneutral plasma circulates in the poloidal plane because the space charge electric field provides a poloidal $\mathbf{E} \times \mathbf{B}$ drift. In a purely toroidal magnetic field, the single particle total energy (in the drift orbit approximation) can be written as

$$U(R,z) = qV(R,z) + \frac{L_z^2}{2mR^2} + \frac{\mu B_o R_o}{R}, \tag{2}$$

where q and m are the particle's charge and mass respectively, V is the electrostatic potential, L_z is the component of the angular momentum about the symmetry axis (z-axis), and μ is the particle's magnetic moment. The first term in Eq. 2 is the potential energy, the second is kinetic energy associated with motion parallel to **B**, and the last term is kinetic energy associated with the gyro-motion perpendicular to **B**. Total energy, angular momentum and magnetic moment are all conserved. As the particle $\mathbf{E} \times \mathbf{B}$ drifts around from the low field (outboard) side of the poloidal plane to the high field (inboard) side, both kinetic energy terms increase at the expense of electrostatic potential energy. The particle moves down the potential energy hill. Closed drift orbits will exist only if the electrostatic potential energy is greater than the change in the particle's kinetic energy as it goes from outboard to inboard. A rough criterion for closing the drift orbits in a toroidal nonneutral plasma is therefore, $qV_s > kT$, where V_s is the space charge potential of the plasma, and kT is the temperature (times Boltzmann's constant).

Consider the difference between charged particle drift orbits in the presence of a substantial space charge and orbits in a field with a rotational transform but no space charge. If the magnetic field possesses a rotational transform, the single particle energy cannot be written in the form of Eq. 2. The (canonical) angular momentum includes a term due the magnetic vector potential (or equivalently the poloidal magnetic flux) and therefore kinetic energy associated with parallel motion, when expressed in terms of the conserved canonical angular momentum, is z- as well as R-dependent. As charged particles flow along the magnetic field from the low field side to the high field side, they gain perpendicular kinetic energy (μ is conserved) at the expense of parallel kinetic energy ($V \approx 0$). Particles with insufficient parallel kinetic energy on the low field side are reflected at the point where parallel kinetic energy vanishes. These are the so-called "trapped particles" in the tokamak with "banana"-shaped drift orbits. In the toroidal *nonneutral* plasma the energy exchange is between electrostatic potential energy and kinetic energy as opposed to an exchange between parallel and perpendicular kinetic energy. Therefore, there are no banana orbits in the nonneutral case.

The equilibrium momentum equation for the electron fluid, neglecting electron inertia and thermal effects, is

$$\mathbf{J} \times \mathbf{B} = -ne\nabla V, \tag{3}$$

where n is the electron density and e is the elementary charge. The cold electron fluid $\mathbf{E} \times \mathbf{B}$ drifts along equipotential contours. Because the plasma is nonneutral, the drift results in a current, $\mathbf{J}$, which when crossed into the magnetic field, $\mathbf{B}$, balances the electrostatic self-repulsion of the plasma. By writing the momentum equation in the form of Eq. 3, its similarity to the magnetohydrodynamic (MHD) equilibrium momentum equation is evident, $\mathbf{J} \times \mathbf{B} = \nabla p$. In MHD theory the diamagnetic current crossed into the magnetic field balances the pressure gradient force. The thermal pressure plays a role in MHD equilibrium theory that is nearly analogous to the electrostatic potential energy density for the electron fluid. Combining Eq. 3 with the steady-state continuity equation and using the form for the toroidal magnetic field (Eq. 1), the electron density can be written as [1]

$$n = \frac{f(V)}{R^2}, \tag{4}$$

where $f(V)$ is an arbitrary function of the potential. Evidently, the electron density must vary along an equipotential contour as $1/R^2$. This result can also be obtained by conserving the number of electrons in a magnetic flux tube ("frozen flux") as the fluid element associated with the flux tube $\mathbf{E} \times \mathbf{B}$ drifts around in the poloidal plane. The area of the flux tube is proportional to R ($A \propto 1/B \propto R$) *and* the length of the flux tube is also proportional to R ($L = 2\pi R$), leading to Eq. 4. Substituting Eq. 4 into Poisson's equation yields a partial differential equation for the electrostatic potential [1] (this equation is the analog of the Grad-Shafranov Equation [12] for toroidal MHD equilibrium).

In the MHD description of toroidal plasma equilibrium, force balance in the major radial ($\hat{R}$) direction must be considered [13]. For example, a toroidal plasma current leads to a magnetic "hoop force" directed away from the z-axis. Also, since the pressure gradient has more surface area to act against on the outboard side, there is an outward force known as the "tire tube" force. Equilibrium is provided by a "vertical" (z-directed) magnetic field, oriented such that the $\mathbf{J} \times \mathbf{B}$ force is inward (toward the z-axis), where $\mathbf{J}$ is the toroidal plasma current. The vertical field can be generated passively by surrounding the plasma with a conducting shell, so that as the plasma expands in the $\hat{R}$ direction image currents arise to provide the vertical magnetic field necessary to establish equilibrium. More commonly the vertical field is applied actively using a set of vertical field coils. The position (and shape) of the plasma equilibrium can be controlled in this way. There are analogous "toroidal" forces for an electron plasma [3]. Electrostatic self-repulsion is the source of a "hoop force," because a charged hoop tends to expand. The electrostatic force also has a larger surface area to act against on the outboard side of a finite aspect ratio torus leading to an electrostatic "tire tube" force. In electron plasmas a *horizontal electric field* plays the role of the MHD vertical magnetic field. An electric field in the $+\hat{R}$ direction exerts an inward force on the plasma opposing the outward hoop and tire tube forces. Bhattacharyya and Avinash [5] investigated not only the required magnitude of the horizontal electric field, but the index of variation in the horizontal field required to avoid certain macroscopic instabilities (involving axisymmetric rigid displacements). The experimental design discussed below incorporates horizontal field electrodes that permit a test of theoretical predictions like those of Bhattacharyya and Avinash.

EXPERIMENTAL DESIGN

The experiment makes use of a novel "partially" toroidal design. Sacrificing some of the symmetry of a completely toroidal trap, charge is injected directly onto field lines tied to the trapping region. The trapping region consists of a 'C'-shaped 335° toroidal arc whose ends are defined by the presence of two grids (Fig. 1). Electrons are injected and trapped by application of suitably timed gate pulses to these grids, in a manner similar to the trapping of nonneutral plasmas in cylindrical Penning-Malmberg traps. During the injection phase, the grid furthest from the electron source (referred to hereafter as the "collector grid") is biased to reflect electrons. Trapping begins when the near grid (referred to hereafter as the "source grid") is biased to shut off the source and isolate the trapped population. After a specified "hold time," the trap is dumped onto a collector by removing the bias from the collector grid. The electron source and the collector are located back-to-back between the two grids, but are not shown in Fig. 1.

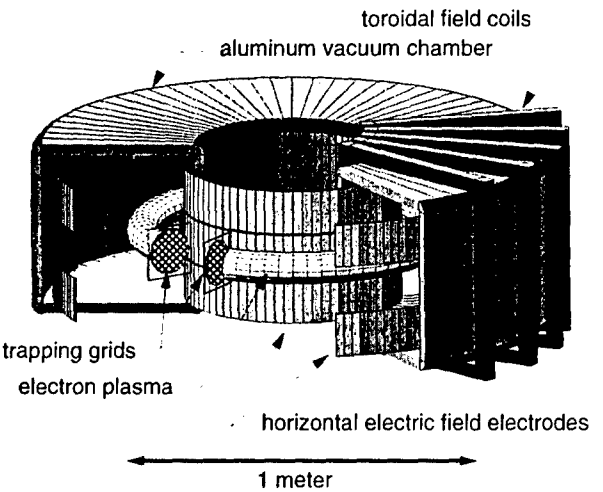

FIGURE 1. Cutaway view of toroidal vacuum chamber showing the trapping grids, horizontal electric field electrodes, a representative set of toroidal field coils and the electron plasma (the electron source and collector reside back-to-back between the grids but are not shown).

The vacuum chamber for this experiment is a 3 cm thick aluminum chamber with a square poloidal cross section [14]. The major radius of the chamber is 50 cm and the poloidal cross-section has inner dimensions of 44 cm by 44 cm. Base pressures of $\sim 2 \times 10^{-7}$ Torr are achieved with a 700 l/s turbomolecular pump, but the pressure rises to $\sim 10^{-6}$ Torr when the tungsten filament (electron source) is heated to its emitting temperature of 1900 K. The toroidal magnetic field coil is composed of 96 turns of 4/0 cable bundled on the outboard side into 24 evenly spaced bundles of 4 turns each. Two interleaved sets of 12 bundles, connected in series, are wound with opposing helicity ensuring that the net toroidal current is zero. The maximum field at the center of the plasma is $B_o \approx 196$ Gauss when the coil is energized with 440 A. The field can be maintained for 30 seconds or more and re-established about every minute without heating the coils significantly.

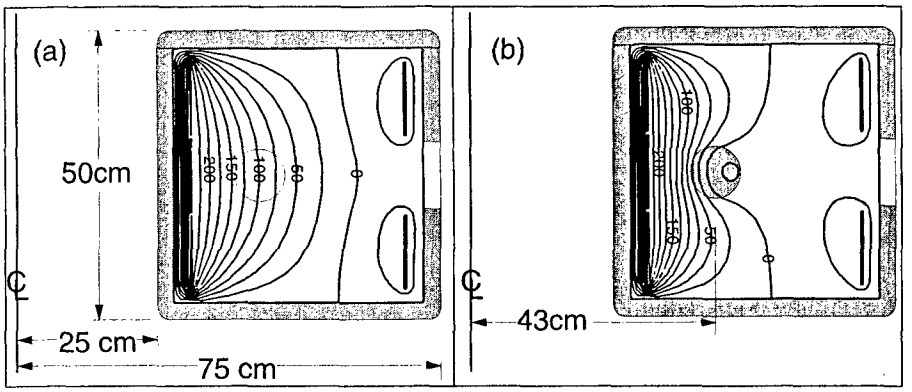

FIGURE 2. A poloidal cross-section of the torus showing (a) the vacuum equipotential contours when +250 V is applied to the inner hoops and -50 V to the outer hoops (contours are spaced every 25 V, open circle indicates location of plasma), and (b) the equipotential contours in the presence of an electron plasma (shaded circle) with average density 3.1×10^6 cm^{-3}.

The electron source is a pancake spiral with 22 turns of 0.5 mm diameter pure tungsten wire. The spiral has a radius of 4.5 cm, the minor radius of the resulting plasma. The center of the filament and the target major radius of the plasma is 43 cm from the major (or z-) axis, a location where the toroidal field ripple is a minimum. Consequently, the plasma is not centered in the chamber, but is 7 cm inboard of the chamber's major radius. The center of the filament is biased to -100 V with respect to its edge, drawing 10.2 A of heating current. The edge of the filament is biased independently with respect to the grounded vacuum chamber. Electrons are drawn from the hot filament by the grounded source grid, a 52% transparent stainless steel grid located 4 cm from the filament. A -250 V potential applied to the source grid suppresses electron flow from the source to the trapping region or vice versa. The collector grid is 252 cm from the source grid as measured along the field. A -300 V potential applied to the collector grid prohibits electron flow from the trapping region to the collector and when +100 V is applied to the grid, the trap contents are dumped. The collector is an aluminum plate biased to +150 V. Collector current is measured with a 1 kΩ sampling resistor.

Five internal stainless steel hoops serve as horizontal electric field electrodes. Three hoops hug the inner wall of the vacuum chamber and the other two are placed above and below the midplane near the outer wall as shown in Fig. 2. Most of the ports are on the outer midplane and the gap between the outer hoops permits diagnostic access, a high conductivity path for pumping, and visual sight lines for inspection of the filament assembly. A typical vacuum equipotential calculation in the poloidal plane is shown in Fig. 2a. While the five hoops can be biased independently, providing control of both the field magnitude and variation across the location of the plasma, for the work reported here the three inner hoops are biased together and the two outer hoops are biased together.

The collector permits diagnosis of the charge remaining in the trap after a specified hold time; however, the measurement requires the destruction of the plasma. An in-

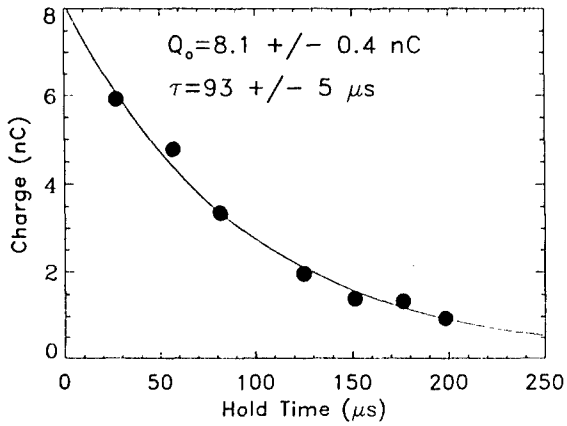

FIGURE 3. Charge (adjusted for trapping grid transparency) dumped onto detector after holding the trap shut for various intervals (circles), and an exponential fit to the data (solid line).

sertable five tip probe can access the plasma *in situ*. The five stainless steel probe tips (1 mm diameter by 3 mm long) are spaced 1.5 cm apart vertically with the middle tip on the midplane. In the work reported here the probe was fixed in position with the middle probe tip 2.5 cm outside the plasma (outboard side). The tips were connected to ground across 11 kΩ, and the flow of image charges across the resistor in response to plasma motion is the signal of interest.

MEASUREMENTS AND RESULTS

To measure the charge confinement time, the trapping grids are cycled through a fill-hold-dump sequence a number of times with different hold times. For each sequence the pulse on the detector is integrated and adjusted for the known transparency of the trapping grid to obtain the total charge leaving the trap. To our knowledge this is the first time the confinement time for a toroidal nonneutral plasma has been measured by the same direct method used in cylindrical Penning-Malmberg traps. Typical results are shown in Fig. 3 (The magnetic field was 196 G at $R = R_o = 43$cm, the inner hoops were biased to +250 V and the outer hoops to -50 V). The charge remaining in the trap decays with a $93 \pm 5\mu$s exponential decay time. By extrapolating the fit back to zero hold time, the maximum trapped charge can be obtained, 8.1 ± 0.4 nC. The trapped charge corresponds to $\sim 5 \times 10^{10}$ electrons and a mean electron density of $(3.1 \pm 0.1) \times 10^6$ cm^{-3}.

The electrostatic potential in the presence of an electron plasma with average density of 3.1×10^6 cm^3 is shown in Fig. 2b. The region of closed potential contours is small compared to the plasma size. Since cold electrons will $\mathbf{E} \times \mathbf{B}$ drift along equipotential

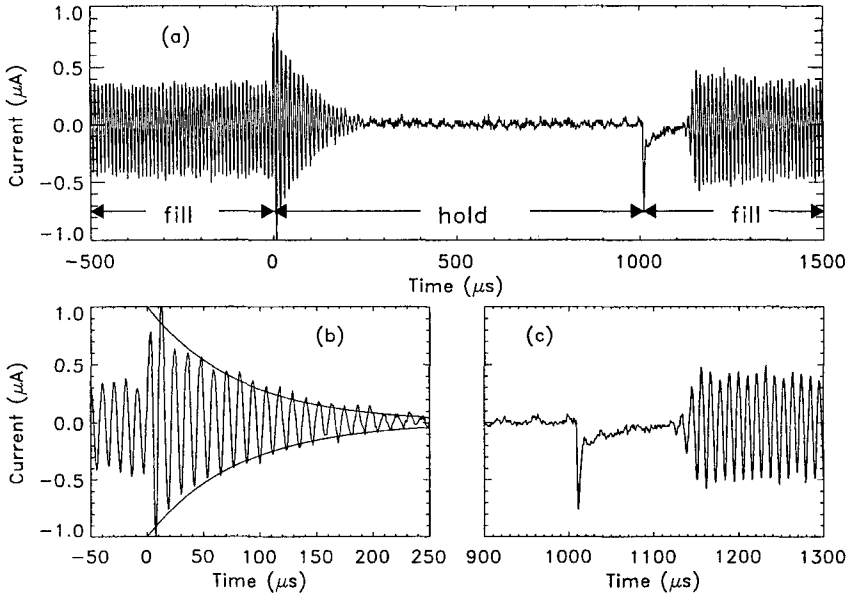

FIGURE 4. Probe signal showing the rate of image charge flow to/from the probe tip (a) while the trap is alternately filled and trapped (trap closes at 0 μs), (b) for times early in the hold phase with an 80 μs exponential decay envelope superimposed on the signal, and (c) for times after the trap is opened showing $\sim 120 - 150\mu$s delay before oscillations reappear.

contours, the region of closed drift orbits for a cold plasma is small. To obtain closed drift orbits that coincide with the location and size of the plasma, substantial curvature drift (or ∇B-drift) effects must be included. Typical electron energies must be 100-200 eV to produce drift orbits consistent with the observed location of the plasma. This energy range is consistent with the acceleration energy given to electrons as they leave the filament, because the center of the filament is at -200 V with respect to ground and the 0 V contour passes near the center of the plasma in this case (Fig. 2b).

Under nearly the same experimental conditions used to obtain the confinement time data in Fig. 3, the flow of image charge signal to and from a probe tip near the plasma is displayed in Fig. 4a. The collector grid was maintained at a steady -400 V while 1 ms long (-250 V) pulses were applied to the source grid. Instead of a fill-hold-dump cycle, this constitutes a fill-hold-fill-hold-... sequence. The hold time is long enough to permit all of the charge to escape before the trap is filled again. There are three features to note in Fig. 4. First, during the fill phase of the cycle ($t < 0$ μs), prior to application of negative trapping bias to the source grid, a large amplitude oscillation is detected on the image charge signal to the probe. The power spectrum for the signal during this phase (Fig. 5a) is dominated by a narrowband feature and its harmonics. Second, when the trap is closed ($t = 0$ μs), the oscillation grows to larger amplitude very quickly and

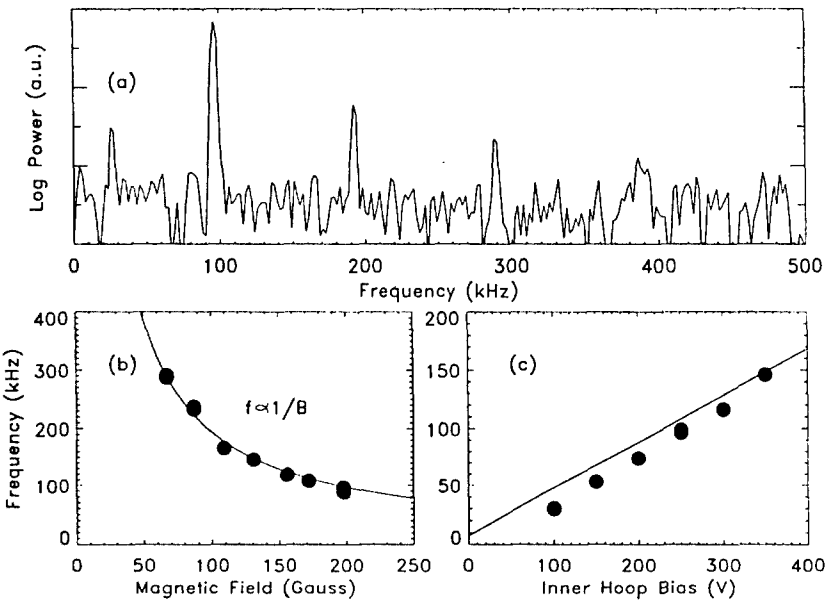

FIGURE 5. The oscillations detected on the probe tip have (a) a power spectrum during fill phase that is dominated by a $\sim$ 100 kHz feature and its harmonics, (b) a fundamental frequency (circles) that is proportional to $1/B$ (solid line is a fit to $1/B$), and (c) a frequency (circles) roughly proportional to the applied horizontal electric field (solid line is E_R/RB_v, where E_R is the calculated vacuum horizontal field).

then decays. The amplitude envelope decays exponentially with a time constant ($\sim$ 80 μs, Fig. 4b) comparable to the confinement time obtained by dumping the trap contents onto the detector (Fig. 3). Note, however, that the oscillation frequency remains constant as the amplitude decays. Third, when the trap is opened again ($t \approx 1000\mu$s), there is delay of about $120 - 150\,\mu$s before the oscillation sets in again (Fig. 4c).

The exponential decay of the oscillation amplitude provides a rapid, alternate method of measuring the confinement time while changing other control variables. Figure 6 shows the decay time constant for the oscillation amplitude as the magnetic field is varied from 67 G to 198 G. The confinement time (as measured by the decay time for the low frequency oscillations) scales roughly as $B^{3/2}$. The scaling differs from the B^2 scaling observed in cylindrical traps both when losses are due to collisions with neutrals [15] and when losses are due to trap asymmetries [16].

The observed low-frequency oscillations are evidently not a straightforward modification of the diocotron modes seen ubiquitously in cylindrical nonneutral plasmas. The longest wavelength diocotron wave (azimuthal mode number $m_\theta = 1$) has a frequency that is proportional to the total charge (per unit length), and shorter wavelength modes have frequencies that are (roughly) proportional to the charge density [17]. The oscillations observed in this experiment maintain a fixed frequency as the plasma decays,

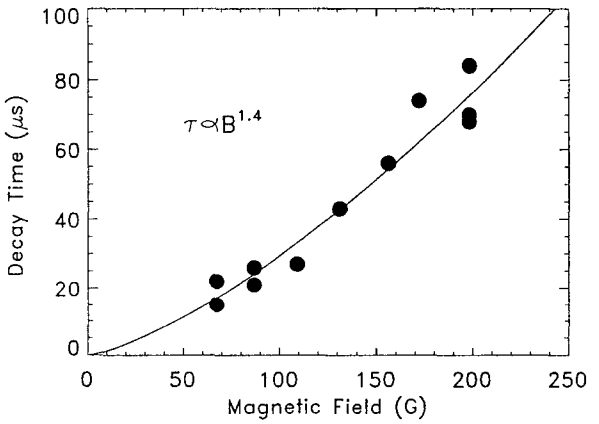

FIGURE 6. The decay time constant for the oscillation amplitude (circles) versus magnetic field, and a power law fit (solid line) with exponent 1.4 ± 0.1.

indicating that the frequency does not depend on the total charge. It is possible that the charge density remains constant as the plasma sheds electrons from its outer surface and that the observed oscillation is a diocotron wave with $m_\theta > 1$. It seems more likely however, that the presence of the applied horizontal electric field introduces a new mode of oscillation not present in the cylindrically symmetric trap. Bhattacharyya and Avinash [5] predict a mode with characteristic frequency in the range of E_R/RB_o, where E_R is the magnitude of the vacuum horizontal electric field. The experimentally measured frequency is proportional to $1/B$ (Fig. 5b), and is nearly proportional to E_R (Fig. 5c). Bhattacharyya and Avinash model the plasma with a charged hoop, neglecting the internal structure of the plasma, and consider only modes of oscillation involving rigid axisymmetric displacements. The magnitude of the horizontal electric field required experimentally to trap electrons ($\sim$ 925 V/m) is much larger than their model predicts for the same total charge ($\sim$ 140 V/m) and the index of variation for the field would make the mode unstable with a purely imaginary frequency. The model evidently needs to be extended to explain our observations.

The $120-150\,\mu$s delay before the oscillations reappear after opening the trap (Fig. 4c) suggests that the catalyst for growth of the oscillations is the accumulation of ions. The neutral pressure (measured with a standard hot filament ion gauge) is in the range $1-2\times10^{-6}$ Torr during these experiments. The residual gas is a mix of molecular hydrogen, water vapor and molecular nitrogen. A typical room temperature proton produced by electron impact ionization of residual gas will drift out of the trap on a $\sim 500\,\mu$s timescale, hence on the timescale of the experiments reported here ions are, for all practical purposes, confined. An order of magnitude calculation suggests that a significant ion population ($\sim$ 10% of n_e) could accumulate in $100\,\mu$s. When the ion orbit frequency resonates with a mode of the electron plasma, the ion resonance instability

sets in [18, 19]. The negative energy electron mode grows by pumping up the ion orbits. At this time we do not have a quantitative understanding of the oscillation frequency or spatial structure.

CONCLUSIONS

Electron plasmas with confinement times as long as 100 μs ($B \approx 200$ G) and densities $n \approx 3 \times 10^6$ cm^{-3} are produced in a partially toroidal trap. Successful trapping requires application of a horizontal electric field as predicted by Bhattacharyya and Avinash [5], although the magnitude of the applied field is significantly larger than theory predicts for a high aspect ratio electron plasma. Drift orbit calculations suggest that typical electron energies are in the range of 100-200 eV. The confinement time is found to scale with magnetic field as $\tau \propto B^{\frac{1}{2}}$, weaker than the B^2 scaling seen in cylindrical traps [15, 16]. Low frequency oscillations are observed with a frequency roughly proportional to E_R/B, where E_R is the vacuum applied horizontal electric field. Some indications point toward the ion resonance instability as the cause of these oscillations [18, 19].

ACKNOWLEDGMENTS

The authors acknowledge the contributions of Angela Kopp. The project is funded by Lawrence University and by grants from Research Corporation (Award No. CC4593) and the U.S. Department of Energy (Grant No. DE-FG02-98ER54503).

REFERENCES

1. Daugherty, J.D. and Levy, R.H., Phys. Fluids **10**, 155 (1967).
2. Elsässer, K., Yu, M.Y., and Shukla, P.K., Phys. Lett. A **152**, 59 (1991).
3. Avinash, K., Phys. Fluids B **3**, 3226 (1991).
4. Hurricane, O.A., Phys. Plasmas **5**, 2197 (1998).
5. Bhattacharyya, S.N. and Avinash, K., Phys. Fluids B **4**, 1702 (1992).
6. Bhattacharyya, S.N. and Avinash, K., Phys. Lett. A **171**, 367 (1992).
7. O'Neil, T.M. and Smith, R.A., Phys. Plasmas **1**, 2430 (1994).
8. Daugherty, J.D., Eninger, J.E., and Janes, G.S., Phys. Fluids **12**, 2677 (1969).
9. Clark, W., Korn, P., Mondelli, A., and Rostoker, N., Phys. Rev. Lett. **37**, 592 (1976).
10. Puravi Zaveri, John, P.I., Avinash, K., and Kaw, P.K., Phys. Rev. Lett. **68**, 3295 (1992).
11. Khirwadkar, S.S., John, P.I., Avinash, K., and Kaw, P.K., Phys. Rev. Lett. **71**, 4334 (1993).
12. Freidberg, J.P. *Ideal Magnetohydrodynamics*, Plenum Press, New York, 1987, pp.75-83.
13. Ibid., p.111.
14. The vacuum chamber was formerly used in the Tokapole II experiment. See for example, Biddle, A.P., *et. al.*, Nucl. Fusion **19**, 1509 (1979).
15. deGrassie, J.S. and Malmberg, J.H., Phys. Fluids **23**, 63 (1980).
16. Driscoll, C.F. and Malmberg, J.H., Phys. Rev. Lett. **50**, 167 (1983).
17. Davidson, R.C. *Physics of Nonneutral Plasmas*, Addison-Wesley, Redwood City, CA, 1990, p. 304.
18. Levy, R.H., Daugherty, J.D., and Buneman, O., Phys. Fluids **12**, 2616 (1969).
19. Peurrung, A.J., Notte, J., and Fajans, J., Phys. Rev. Lett. **70**, 295 (1993).